Emergence of chiral spin liquids via quantum melting of noncoplanar magnetic orders

Ciarán Hickey,[1] Lukasz Cincio,[2,3] Zlatko Papić,[4] and Arun Paramekanti[1,5]

[1]*Department of Physics, University of Toronto, Toronto, Ontario M5S 1A7, Canada*
[2]*Theoretical Division, Los Alamos National Laboratory, Los Alamos, New Mexico 87545, USA*
[3]*Perimeter Institute for Theoretical Physics, Waterloo, Ontario N2L 2Y5, Canada*
[4]*School of Physics and Astronomy, University of Leeds, Leeds, LS2 9JT, United Kingdom*
[5]*Canadian Institute for Advanced Research, Toronto, Ontario M5G 1Z8, Canada*

Quantum spin liquids (QSLs) are highly entangled states of quantum magnets which lie beyond the Landau paradigm of classifying phases of matter via broken symmetries. A physical route to arriving at QSLs is via frustration-induced quantum melting of ordered states such as valence bond crystals or magnetic orders. Here we show, using extensive exact diagonalization (ED) and density-matrix renormalization group (DMRG) studies of concrete $SU(2)$ invariant spin models on honeycomb, triangular, and square lattices, that chiral spin liquids (CSLs) emerge as descendants of triple-Q spin crystals with tetrahedral magnetic order and a large scalar spin chirality. Such ordered-to-CSL melting transitions may yield lattice realizations of effective Chern-Simons-Higgs field theories. Our work provides a distinct unifying perspective on the emergence of CSLs and suggests that materials with certain noncoplanar magnetic orders might provide a good starting point to search for CSLs.

Quantum spin liquids (QSLs) are phases of matter which defy a classical Landau description in terms of broken symmetries and local order parameters [1,2]. Unlike magnetically ordered phases, which can be described using simple mean field wave functions with short-range entanglement, QSLs are highly entangled and feature unusual excitations with fractional quantum numbers. This leads to robust many-body properties of QSLs which are of potential use in topological quantum memories and quantum computation [3].

In this paper, we focus on two-dimensional (2D) chiral spin liquids (CSLs), close cousins of the celebrated fractional quantum Hall states. CSLs exhibit topological ground state degeneracies, possess gapped anyonic excitations, and were originally proposed by Kalmeyer and Laughlin in 1987 [4] as candidate ground states of the spin-1/2 triangular lattice Heisenberg antiferromagnet (although this model Hamiltonian is now known to have long-ranged magnetic order). Specifically, viewing the spins as hard-core bosons, the Kalmeyer-Laughlin state is equivalent to a $\nu = 1/2$ bosonic Laughlin liquid with gapped semion excitations. This is the particular CSL that we will focus on in the rest of this paper.

The surge of recent interest in such CSLs started with the introduction of parent Hamiltonians or exactly solvable models [5–8], as well as numerical studies of a variety of simple frustrated spin models which yielded CSL ground states on the kagome [9–18], square [19–21], honeycomb [22], and triangular lattices [23,24]. CSLs have also been described using variational Gutzwiller projected fermion or boson wave functions, whose low energy properties are captured in terms of spin-1/2 partons (spinons) coupled to emergent dynamical gauge fields. From this perspective, we can obtain the CSL ground state by starting with spin-1/2 fermions filling up individual Chern bands with $C = 1$, leading to an integer quantum Hall state with $\sigma_{xy}^{\text{total}} = 2e^2/h$, and Gutzwiller projecting this state (which enforces the constraint of one fermion per site) to yield a legitimate spin wave function [25–28], A complementary picture is to view them as Gutzwiller projected integer quantum Hall states of strongly interacting bosons

with $\sigma_{xy} = 2e^2/h$ [29–35]. Gutzwiller projection promotes the global $U(1)$ symmetry of the fermions or bosons to a local gauge invariance, leading to an emergent low energy $U(1)_2$ Chern Simons theory.

A physically different way to think about QSLs is to start from broken symmetry phases of $SU(2)$ magnets and introducing strong quantum fluctuations to melt the long-range order. For instance, certain frustrated quantum magnets support ordered crystals of valence bond singlets between nearby spins. However, quantum fluctuations of such singlet dimers can melt the crystalline order, resulting in a quantum superposition of dimer configurations, which provides the resonating valence bond description of gapped Z_2 QSLs [36]. We can also arrive at such a QSL by quantum disordering a coplanar spin spiral, without simultaneously proliferating Z_2 vortices which are topological point defects in the magnetically ordered phase [37].

Here, we focus on the question of how to realize CSLs from quantum disordering magnetically ordered states. We consider previously discovered $SU(2)$ invariant CSLs on honeycomb, triangular, and square lattices and use extensive numerical exact diagonalization (ED) and density matrix renormalization group (DMRG) calculations [38,39] to show that they descend from parent noncoplanar magnetic orders with zero net magnetization and a nonzero scalar spin chirality. Such noncoplanar magnetism arises, for instance, in skyrmion crystal phases. Our work thus presents a distinct unifying perspective on such chiral spin liquids and suggests that Mott insulators with noncoplanar magnetic orders might be viable candidates for realizing chiral spin liquids—by tuning exchange couplings via physical pressure or chemical composition in order to melt the magnetic order.

Our study relies crucially on the classification of so-called "regular magnetic orders" (RMOs): magnetically ordered states which preserve all lattice symmetries modulo global spin rotations [40]. (We note that the original classification of classical RMOs considered orders which preserved all lattice symmetries up to global spin rotations and spin inversion

$\mathbf{S} \rightarrow -\mathbf{S}$. However, spin inversion is not a symmetry for quantum spins or even a classical symmetry in the presence of chiral interactions, so we drop spin inversion in our definition of RMOs.) If we start from such a RMO, and introduce strong quantum fluctuations and frustration, we might expect to restore a fully symmetric liquid state of spins. This suggests that RMOs with noncoplanar order, net zero magnetization, and a large net scalar spin chirality are likely to be natural candidates for parent states of singlet CSLs.

As an example, we have recently studied the phase diagram of an extended Heisenberg model on the honeycomb lattice with additional chiral spin interactions [22] and found that the CSL emerges in proximity to a tetrahedral state, which is a noncoplanar RMO. Similar results were subsequently found in a triangular lattice spin model [24]. Here, we present careful ED and DMRG calculations of the fidelity and energy in these two models, which show that the tetrahedral state and the CSL appear to be separated by a continuous rather than a first-order transition. This signifies that the CSL may be viewed as descending from the tetrahedral state on both lattices. Interestingly, such tetrahedral orders and the possibility of topological phases arising from them was pointed out in previous work on itinerant fermion models [41–44].

We next turn to the square lattice, for which there are *no* noncoplanar RMOs (as we define it). However, if we allow for C_4 symmetry breaking, it turns out there is a noncoplanar RMO with net zero magnetization, which is a distorted 'tetrahedral umbrella' state. We therefore focus here on Hamiltonians on the square lattice which explicitly break the C_4 symmetry of the Hamiltonian, by including a staggered chiral interaction. This does not impact the topological order of the CSL, since it should survive even in the presence of such symmetry breaking. However, the simplification is that at the transition from the magnetically ordered state to the CSL, we only need to restore spin rotation symmetry while inducing topological order, similar to the triangular and honeycomb lattice examples. Indeed, we find that in this case, the combination of staggered chiral interaction and a further neighbor Heisenberg coupling again drives what appears to be a continuous quantum phase transition between a tetrahedral umbrella state and a square lattice CSL.

We conjecture that the phases and the seemingly direct phase transitions between them which we have uncovered in our numerical studies may provide microscopic realizations of Chern-Simons-Higgs field theories. In this scenario, the CSL is the phase with gapped matter fields (bosonic spinons) minimally coupled to a $U(1)_2$ Chern Simons gauge theory in its deconfined phase, while the ordered phase is a Higgs condensate of spinons which leads to noncoplanar magnetic order and a simultaneous loss of topological order.

I. MODEL HAMILTONIANS

The models we study in this paper are $SU(2)$ invariant spin Hamiltonians with extended Heisenberg interactions, supplemented by a chiral three-spin interaction:

$$H_{\rm spin} = \frac{1}{2} \sum_{i,j} J_{i,j} \mathbf{S}_i \cdot \mathbf{S}_j + J_\chi \sum_{i,j,k \in \triangle} \mathbf{S}_i \cdot (\mathbf{S}_j \times \mathbf{S}_k). \quad (1)$$
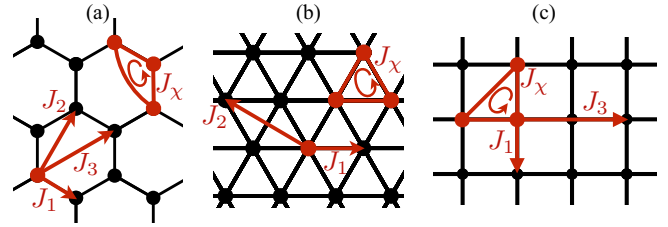

FIG. 1. Heisenberg exchange J_α and scalar spin chirality J_χ interactions used in the text for the (a) honeycomb, (b) triangular, and (c) square lattice.

Here, as indicated in Fig. 1, the extended Heisenberg interactions include the first few neighbors, while $\sum_{\triangle}$ in the chiral interaction denotes a sum over the smallest triangular plaquettes, with $\{i,j,k\}$ taken anticlockwise around the triangle.

We emphasize that the chiral terms, which explicitly break time-reversal symmetry, are not necessarily crucial for realizing CSLs; indeed, it has been shown on the kagome lattice that a CSL with spontaneous breaking of time-reversal symmetry can be realized in an extended Heisenberg model [13]. Nevertheless, we retain them since models including such chiral terms have been shown to realize CSLs on most 2D lattices—honeycomb, triangular, square, and kagome—and our main aim here is to relate these CSLs to underlying parent magnetic orders.

If we start from a Hubbard model (with hoppings $t_{i,j}$ and local repulsion U) and attempt to derive $H_{\rm spin}$ as an effective spin Hamiltonian in the Mott limit, we find $J_{i,j} = 4t_{ij}^2/U$, while the chiral interaction is $J_\chi = 24(t^3/U^2) \sin \Phi_\triangle$ if the Hubbard model has nonzero orbital fluxes $\Phi_\triangle$ penetrating the triangular plaquettes. Such chiral terms have been suggested to be relevant for understanding orbital magnetic field effects in certain organic spin liquids [45] and for interacting ultracold atomic systems with 'artificial' gauge fields (where models such as the honeycomb lattice Haldane model of a quantum anomalous Hall insulator have been experimentally realized [46,47]). More recently, there has been a very interesting suggestion to induce such chiral terms via circularly polarized light rather than by an orbital magnetic field [48,49]. The Hubbard model derivation suggests that the chiral terms will greatly influence magnetism in the 'weak' Mott insulator regime $U \gtrsim t$. However, as $U/t \rightarrow \infty$, i.e., deep in the Mott insulator regime, the chiral terms will become less important than two-spin interactions. In our study we will treat this Hamiltonian $H_{\rm spin}$ simply as a spin model in its own right.

II. NUMERICAL SIGNATURES

Within an ED calculation, a CSL and a magnetically ordered state can be distinguished by their low-lying energy spectrum and the static spin structure factor of their ground state. In a magnetically ordered state, with net zero magnetization, the first excited state should be a spin triplet with momenta associated with the magnetic ordering wave vectors. It forms part of the "Anderson tower of states" that lead to a symmetry broken ground state in the $N \rightarrow \infty$ limit [50,51]. The static spin structure factor of the ground state, $\mathcal{S}(\mathbf{q}) = \frac{1}{N} \sum_{i,j} \langle \mathbf{S}_i \cdot \mathbf{S}_j \rangle e^{i\mathbf{q} \cdot (\mathbf{r}_i - \mathbf{r}_j)}$, should display clear peaks

at the expected ordering wave vectors. On the other hand, in the CSL phase, both the ground state and the first excited state should be spin singlet states with momentum $\mathbf{k} = (0,0)$ on all of the lattices studied here ($L_x \times L_y$ lattices with both L_x and L_y even, and periodic boundary conditions). The gap between these two states should vanish in the $N \to \infty$ limit so that they form the degenerate ground state manifold (GSM) of the topologically ordered CSL on the torus. The static spin structure factor of the ground state should be featureless, with no sharp peaks, indicative of a magnetically disordered state.

Our DMRG calculations are done in the infinite cylinder limit [52,53] with varying circumferences L_y. Within such DMRG calculations, one indicator that we are in a CSL is that we are able to find multiple distinct ground states associated with the topological order. By contrast, in regimes where we expect magnetic order, we always find only a single ground state. A more positive indicator is to calculate the total quantum dimension which is encoded in the overlap of a single ground state on a torus $|\Psi_i\rangle$ with its rotated version, i.e., $R_{ii} = \langle\Psi_i| \mathcal{R}_{\pi/3} |\Psi_i\rangle$. Here, $\mathcal{R}_{\pi/3}$ denotes $\pi/3$ rotation of a state on a torus (the appropriate rotation for a lattice with C_6 symmetry). In an Abelian topologically ordered phase with total quantum dimension D, we expect $|R_{ii}| = 1/D$, with $D = \sqrt{2}$ for a CSL. In a topologically trivial state, however, we expect $|R_{ii}| = 1$. As a more complete characterization, we can also study the S and T matrices of the anyons in the topologically ordered state by constructing the matrix $R_{ij} = \langle\Psi_i| \mathcal{R}_{\pi/3} |\Psi_j\rangle$ of overlaps between all pairs of states in the GSM [54]. However, this is not something that we can track across the transition. Yet another distinction between the CSL and magnetically ordered states lies in the edge entanglement spectrum obtained by cutting the cylinder into two halves, with the CSL showing a signature of a free chiral boson described by an $SU(2)_1$ Wess-Zumino-Witten (WZW) conformal field theory [54].

To probe the nature of the transition between the CSL and the magnetically ordered states, we calculate the ground state energy per spin and the ground state fidelity, usually defined as $F(g) = |\langle\Psi(g)|\Psi(g + \delta g)\rangle|$, where the ground state $|\Psi(g)\rangle$ is parameterized by the tuning parameter g. The fidelity has been shown to be an indicator of quantum phase transitions, both symmetry-breaking transitions as well as certain topological phase transitions [55,56]. A first order transition is signalled by a sharp discontinuity in F, which jumps to zero at the transition where there is a ground state level crossing. By contrast, a continuous transition is signalled by a weak dip in F at the transition, which results in a (more clearly visible) peak in the fidelity susceptibility $\chi^F(g) = \partial^2 F(g)/\partial g^2$. In the case of topologically ordered states the ground state is not unique so we instead define a GSM fidelity. If the states in the GSM do not mix with one another and there are no exact degeneracies (both of which are conditions satisfied in the models and clusters studied here using ED), then we can define the GSM fidelity for an n-fold degenerate GSM as

$$F_n(g) = \frac{1}{n} \sum_{i=1}^{n} |\langle\Psi_i(g)|\Psi_i(g + \delta g)\rangle|, \qquad (2)$$

where $n = 2$ for the CSL. Associated with this, we define the fidelity susceptibility $\chi_n^F = \partial^2 F_n/\partial g^2$, which we compute as

the numerical second derivative of the fidelity

$$\chi_n^F = \frac{F_n(g + \delta g) - 2F_n(g) + F_n(g - \delta g)}{(\delta g)^2}. \qquad (3)$$

In ED, we study F_2 and χ_2^F since we can track the two states that make up the GSM in the CSL, GS1 and GS2, throughout the phase diagram, i.e., we can adiabatically follow the two CSL ground states even into the topologically trivial phase (where the upper of the two states in the GSM levitates into a genuine excited state). In the DMRG calculations, however, we do not have access to this second state in the topologically trivial phase. We thus compute the fidelity F of just a single GS; in the CSL, this corresponds to tracking that ground state which is adiabatically connected to the unique ground state we find in the topologically trivial phase.

III. RESULTS

Below, we discuss the results we obtain from both ED and DMRG studies for the honeycomb, triangular, and square lattices. We defer a discussion of the kagome lattice CSL to a future publication. The data presented is from the largest system sizes studied. For ED this is $N = 32$ sites for the honeycomb lattice and $N = 36$ sites for the triangular and square lattices. In the DMRG simulations we studied infinite cylinders of width up to six lattice unit cells for honeycomb and triangular lattices. We keep at most $\chi = 2048$ states in the infinite DMRG algorithm, finding convergence in all quantities of interest. χ is referred to as bond dimension throughout the remaining part of the text. Results on smaller clusters are consistent with the conclusions presented here.

A. Honeycomb lattice

For the honeycomb lattice, we keep Heisenberg terms, J_1, J_2, J_3 corresponding to first, second, and third nearest neighbors, in addition to the chiral term J_χ, as shown in Fig. 1(a). Our recent study of this model found a tetrahedral phase in this model for $J_3 = 0$ and a CSL phase for sufficiently large $J_3 > 0$. Here, we fix $J_1 = 1.0$, $J_2 = 0.36$, and $J_\chi = 0.31$ and use ED and DMRG to investigate the nature of the transition between the tetrahedral state and the CSL state upon increasing J_3.

In ED, for small $J_3 \geqslant 0$, we find that the ground state is a spin singlet, with large uniform ground state spin chirality $\langle\mathbf{S}_i \cdot \mathbf{S}_j \times \mathbf{S}_k\rangle \sim 0.16$ on the small triangles of the honeycomb lattice [shown in Fig. 1(a)] consistent with strong noncoplanarity of the spins. The first excited state is a spin triplet with momenta at the M points, the ordering wave vector of the tetrahedral state, and the static spin structure factor, shown in Fig. 2(a) for $J_3 = 0.04$, also exhibits clear peaks at the M points. The full spectrum, shown in our previous study (see Supplemental Material of Ref. [22]), exhibits an 'Anderson tower' consistent with a noncoplanar ground state having fully broken spin rotational symmetry. All these are clear signatures of the triple-Q tetrahedral state.

By contrast, at $J_3 = 0.36$, we find that the system is in the CSL phase. At this point, ED shows that both the ground state and the first excited state are spin singlet states with momentum $\mathbf{k} = (0,0)$, and they are well separated by a gap
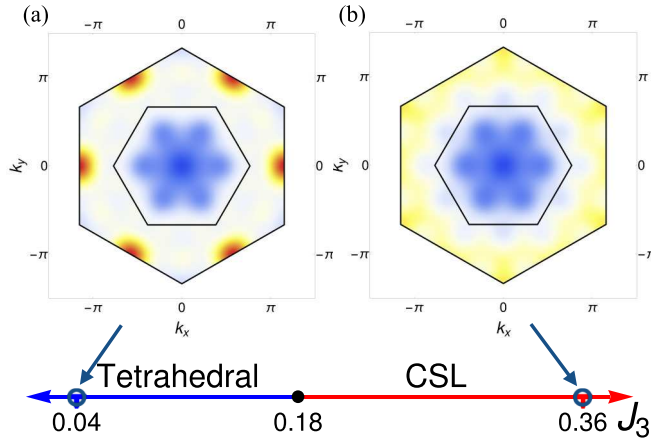
FIG. 2. Phase diagram of the honeycomb lattice model for $N = 36$ sites as a function of J_3 for fixed $J_1 = 1.0$, $J_2 = 0.36$, $J_\chi = 0.31$. The static spin structure factor, $S(\mathbf{q})$, of the ED ground state for $N = 32$ sites is shown for the (a) tetrahedral and (b) CSL phases. $S(\mathbf{q})$ exhibits sharp peaks at the M points of the (second) BZ in the tetrahedral state but not in the CSL state.

from all other excitations [22]. The energy splitting between these two lowest states decreases as system size increases, being 0.16, 0.11, and 0.03 on 18, 24, and 32-site clusters, respectively. This is consistent with a twofold topological ground state degeneracy on the torus in the thermodynamic limit, and we have confirmed this by computing the many-body Chern number using flux threading [22]. In addition, the static spin structure factor, shown in Fig. 2(b), exhibits no sharp peaks, indicating short-ranged spin correlations.

As a further indication that there is a topological phase transition, DMRG always finds two ground states at $J_3 = 0.36$. For either ground state $|\Psi_i\rangle$, the overlap $|\langle\Psi|\mathcal{R}_{\pi/3}|\Psi\rangle| \approx 1/\sqrt{2}$ for various bond dimensions as shown in Fig. 3(d). This indicates that it is consistent with a topologically ordered CSL having total quantum dimension $D = \sqrt{2}$. Figure 3(b) shows the DMRG edge entanglement spectra in the CSL phase (here, we have picked one of the two ground states), which clearly resembles that of a free chiral boson. In our previous study of this model, we have provided further evidence for the CSL phase, including the full S and T matrices. We contrast these observations with the results at $J_3 = 0.04$. Here, we only find a single ground state, with the overlap $|\langle\Psi|\mathcal{R}_{\pi/3}|\Psi\rangle|$ extrapolating to 1 with increasing bond dimension χ as shown in Fig. 3(c), indicative of a topologically trivial phase. Upon decreasing J_3, and entering the tetrahedral state, we find many additional low-lying states in the entanglement spectrum as seen from Fig. 3(a), leading to a complete breakdown of the free chiral boson description.

Taken together, these results provide clear evidence that, somewhere between $J_3 = 0.04$ and $J_3 = 0.36$, there must be a phase transition between a magnetically ordered tetrahedral phase and the CSL. In order to study this transition, we have computed the energy per site as well as the fidelity and fidelity susceptibilities with varying J_3. As shown in Fig. 4(a), the energy shows no sharp kinks, suggesting that this transition is not obviously first order. Similarly the fidelity of the ground states from ED and DMRG shown in Fig. 4(b) are smooth,
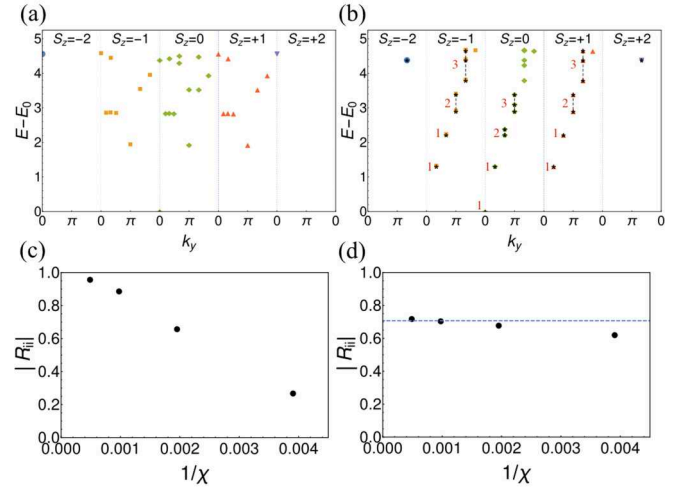

FIG. 3. The edge entanglement spectrum obtained using DMRG for the honeycomb model is shown in the (a) tetrahedral ground state and (b) one of the two CSL ground states showing the free chiral boson spectrum. The overlap $|R_{ii}| = |\langle\Psi_i|\mathcal{R}_{\pi/3}|\Psi_i\rangle|$ for various bond dimensions χ is shown in (c) the tetrahedral phase, where it extrapolates to $|R_{ii}| = 1$, and (d) the CSL phase, where it extrapolates to $|R_{ii}| = 1/\sqrt{2}$ (the dashed blue line).

again suggesting a continuous transition. χ_2^F, computed using ED, has a clear peak at $J_3 = 0.18$, which we take to be the transition point for the $N = 32$ site system. In summary, our
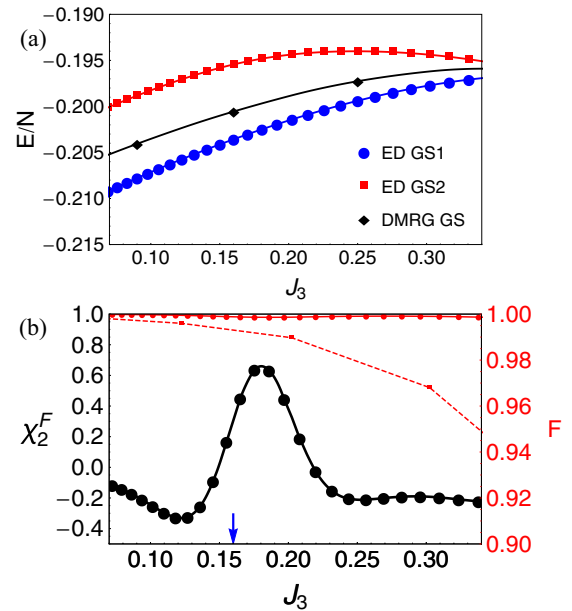

FIG. 4. (a) Energy per site for the honeycomb model of a single ground state from DMRG and of the two states from ED that make up the ground state manifold of the CSL. (b) Fidelity of a single ground state from DMRG (dashed red line) and of the ground state manifold from ED (solid red line). The decrease in the DMRG fidelity with increasing J_3 is due to the nearby CSL-Néel transition at even larger J_3. The fidelity susceptibility from ED (solid black line) shows a clear peak at $J_3 = 0.18$, signifying the transition from the tetrahedral to CSL. The arrow indicates the position at which the first excited state has a level crossing, switching from a triplet at the M point in the tetrahedral phase to a singlet at the Γ point in the CSL.

ED and DMRG results indicate that the tetrahedral state may be viewed as a parent magnetically ordered state from which the CSL descends via a seemingly continuous transition upon increasing frustration through $J_3 > 0$.

B. Triangular lattice

For the triangular lattice, we consider a model with nearest and next-nearest neighbor Heisenberg terms J_1, J_2, supplemented by a nonzero J_χ. For fixed $J_1 = 1.0$, the phase diagram of the model has already been determined using ED (with up to 36 spins) over a range of couplings $0 \leqslant J_2 \leqslant 0.3$ and $0 \leqslant J_\chi \leqslant 0.6$. Among other phases, a CSL phase was found bordering a magnetically ordered tetrahedral phase. Here, we fix $J_\chi = 0.4$ and vary J_2 in order to investigate the nature of the transition from the CSL to the tetrahedral.

At $J_2 = 0.15$, the system is in a tetrahedral state. Our ED results show that the ground state is a singlet while the first excited state is a spin triplet with momentum at the M point. The static spin structure factor of the ground state, shown in Fig. 5(b), has clear peaks at the M points. At the same time, DMRG finds a single ground state, indicative of a topologically trivial phase.

At $J_2 = 0.0$, the system is in the CSL phase. In ED, both the ground state and the first excited state are spin singlet states with momentum $\mathbf{k} = (0,0)$. The static spin structure factor of the ground state, shown in Fig. 5(a), has no sharp peaks. Furthermore, in DMRG we find two distinct ground states indicative of topological order, and the entanglement spectrum resembles that of a free chiral boson, as shown in Fig. 5(c). Upon increasing J_2, and entering the tetrahedral state, we again find many additional low lying states [highlighted in Fig. 5(d)], leading to strong deviations from the free chiral boson description.
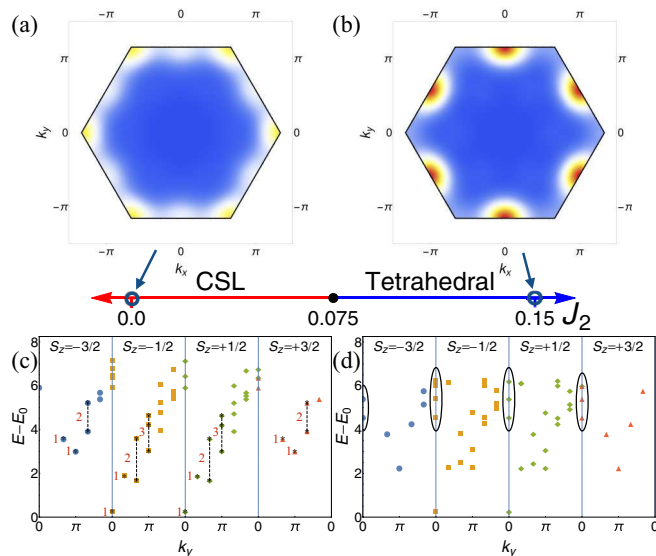

FIG. 5. Phase diagram of the triangular lattice model for $N = 36$ sites as a function of J_2 for fixed $J_1 = 1.0$, $J_\chi = 0.4$. The static spin structure factor of the ED ground state for $N = 36$ spins is shown for the (a) CSL and (b) tetrahedral phases. The DMRG edge entanglement spectra in (c) the CSL phase, showing the free chiral boson spectrum and (d) the tetrahedral phase, where the additional low-lying states are highlighted.
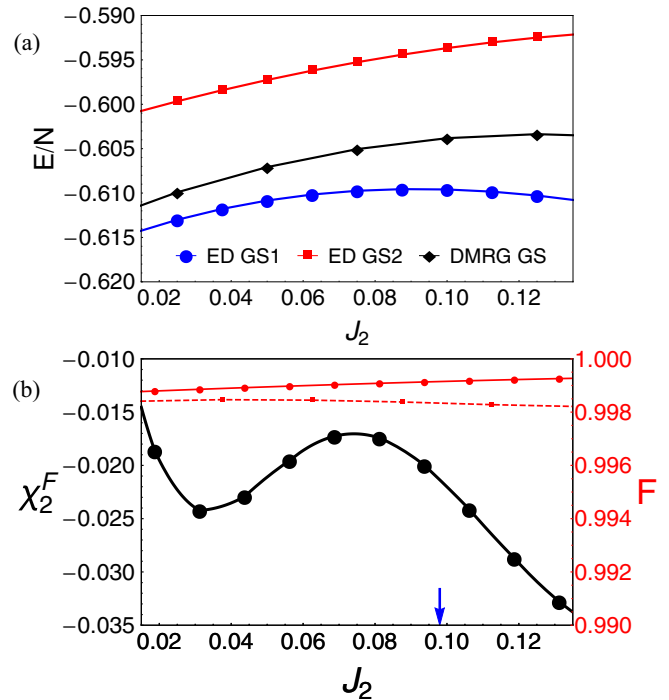

FIG. 6. (a) Energy per site for the triangular lattice model of a single ground state from DMRG and the two states from ED that make up the ground state manifold of the CSL. (b) Fidelity from DMRG (dashed red line) and ED (solid red line) and fidelity susceptibility from ED (solid black line). The transition is signified by a peak in the fidelity susceptibility at $J_2 = 0.075$. The arrow indicates the position at which the first excited state has a level crossing, switching from a singlet at the Γ point (CSL) to a triplet at the M point (tetrahedral).

Again these results indicate that there must be a phase transition between the CSL and a magnetically ordered tetrahedral phase between $J_2 = 0.0$ and $J_2 = 0.15$. However, the energy of the ground states in ED and DMRG shown in Fig. 6 show no sharp kinks and the fidelities are again smooth. It is only the fidelity susceptibility that provides a signal of the transition, with a broad peak centered at $J_2 = 0.075$. We thus again conclude that the CSL to tetrahedral transition is likely to be continuous, as indicated by our ED and DMRG signatures.

We note that the signatures of the CSL, such as the structure of the entanglement spectrum, are not quite as clean here as in the honeycomb lattice case. This can be explained by the fact that the correlation length ξ_{TM}, extracted from DMRG [57], is shorter for the honeycomb lattice case. The correlation length for the honeycomb lattice at $J_3 = 0.36$ is $\xi_{TM} = 0.88$ whereas for the triangular case at $J_2 = 0.0$ it is more than double at $\xi_{TM} = 1.89$. Here, ξ_{TM} denotes the transfer matrix correlation length defined as $\xi_{TM} = -1/\log(\lambda_2)$, where λ_2 is the second largest eigenvalue of the transfer matrix. The transfer matrix contains tensors associated to one column of an infinite cylinder. ξ_{TM} is the upper bound for any correlation length in the system. The above values for ξ_{TM} are extrapolated in the bond dimension.

C. Square lattice

The square lattice J_1, J_2 model with a nonzero J_χ has already been shown to realize a CSL phase [19]. Here, for
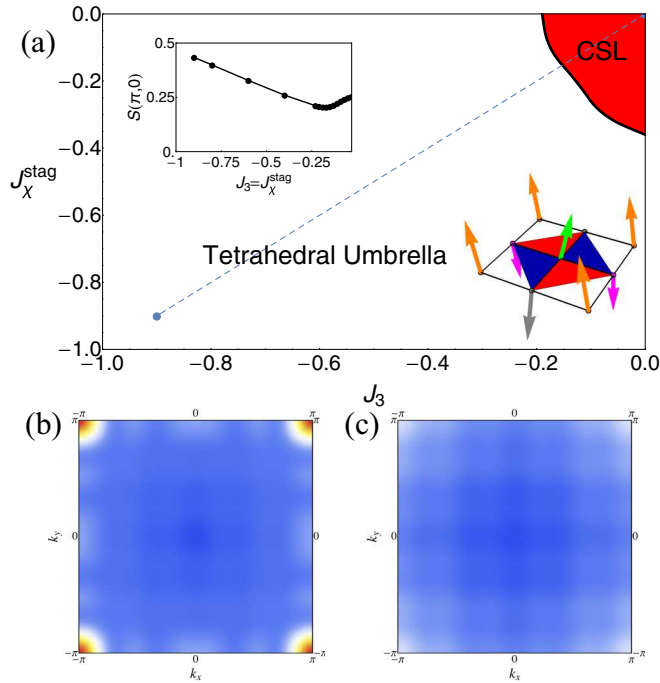
FIG. 7. (a) Phase diagram of the square lattice model for $N = 36$ sites as a function of J_3 and J_χ^{stag} for fixed $J_1 = J_\chi = 1.0$. The inset shows the evolution of the structure factor peak at $X = (\pi,0),(0,\pi)$ along the dashed line. The static spin structure factor of the ED ground state for $N = 36$ spins is shown for the (b) tetrahedral and (c) CSL phases.
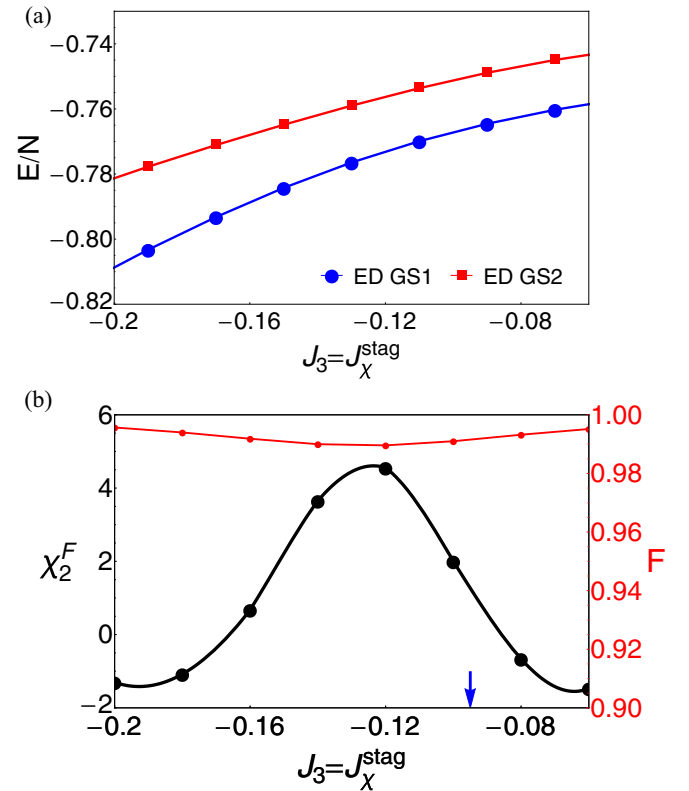

FIG. 8. (a) Energy of the two states from ED that make up the ground state manifold of the CSL for the square lattice model. (b) Fidelity (solid red line) and fidelity susceptibility (solid black line) from ED with the peak in the fidelity susceptibility at $J_3 = -0.125$ marking the transition from the CSL to the tetrahedral. The arrow indicates the position at which the first excited state switches from a singlet at the Γ point to a triplet at the K point.

simplicity, we set $J_1 = J_\chi = 1.0$, and $J_2 = 0$, which places us in the CSL phase. On the square lattice, there are no noncoplanar RMOs. However, allowing for the breaking of C_4 symmetry about a lattice site allows for a noncoplanar RMO which is called the 'tetrahedral umbrella' state, depicted schematically in Fig. 7(a). This state is a multimode spin crystal formed by wave vectors at the $K = (\pi,\pi)$ and $X = (\pi,0),(0,\pi)$ points of the BZ. In addition to breaking spin rotational symmetry, the broken C_4 rotational symmetry about the square lattice sites leads to a staggered modulation of the scalar spin chirality. In order to simply access this phase from the CSL, we add a ferromagnetic third neighbor Heisenberg term $J_3 < 0$ as well as a staggered chiral term J_χ^{stag} that explicitly breaks the square lattice C_4 symmetry, giving a total chiral interaction $J_\chi + J_\chi^{\text{stag}}$ on half of the triangles and $J_\chi - J_\chi^{\text{stag}}$ on the other half. This leads to the phase diagram depicted schematically in Fig. 7(a).

For $J_3 = J_\chi^{\text{stag}} = 0$ the system is in the CSL phase. As before, the ED ground state and the first excited state are spin singlet states with momentum $\mathbf{k} = (0,0)$, and they form the GSM of the CSL, which are reasonably well separated from all the other excited states (with the separation increasing with increasing system size [19]). The static spin structure factor of the ground state, shown in Fig. 7(c), is featureless. For significant $J_3 < 0$ and J_χ^{stag}, on the other hand, the system resembles the tetrahedral umbrella state. In ED, the ground state is a singlet while the first excited state is now a spin triplet with momentum at the $K = (\pi,\pi)$ point, followed by slightly higher energy triplet excitations at the $X = (\pi,0),(0,\pi)$ points.

The static spin structure factor of the ground state, shown in Fig. 7(b), has a sharp peak at the K point and smaller peaks at the X points. These suggest multimode order associated with the tetrahedral umbrella state.

In Fig. 8, we plot the energy per site which is smooth and the GSM fidelity from ED which has a weak dip indicating the transition, with a clear peak in the fidelity susceptibility at $J_3 = -0.125$. Just as in the honeycomb and triangular lattice, the CSL to tetrahedral transition does not show any signatures of first order behavior, supporting the idea that it is again a continuous transition.

IV. DISCUSSION

We have provided numerical evidence (using ED and DMRG) that CSLs on the honeycomb, triangular, and square lattices arise from melting ordered noncoplanar spin crystal states via continuous transitions. This suggests that quantum melting such noncoplanar states is likely to be a general mechanism to obtain CSLs. In previous work, we have conjectured a possible Chern-Simons-Higgs theory which could possibly capture the tetrahedral-CSL transition on the honeycomb lattice. Our work motivates a further study of this exotic continuous transition, including a comparison with the

gauge theory spectrum on the torus which has been studied within a large-$\mathcal{N}$ approximation [58].

There are a number of interesting extensions of this work to consider. In particular it is natural to ask whether this kind of mechanism could be extended to 3D lattices. Can quantum melting a 3D noncoplanar magnetic state lead to a stacked chiral spin liquid state? This may be of relevance to the 3D pyrochlores $Pr_2Ir_2O_7$, which appears to exhibit an anomalous Hall effect without long-range magnetic order, suggestive perhaps of a spin liquid state with nonzero scalar spin chirality [59], and $Lu_2Mo_2O_5N_2$, which has been theoretically identified as a candidate for a molten version of a chiral noncoplanar spiral state [60]. Another interesting direction would be to explore higher spin systems. On the ordered side, moving to higher spin allows for a richer set of order parameters, such as quadrupolar order in the case of spin-1. On the CSL side, higher spin CSLs can have non-Abelian topological order and thus a more complex GSM structure [7,61–64]. Is it possible to find an ordered "parent state" for these higher spin non-Abelian CSLs?

Note added. Recently, we became aware of two preprints [65,66] that also discuss the J_1-J_2-J_χ model on the triangular lattice. Our results are consistent where there is overlap.

ACKNOWLEDGMENTS

[1] Y. Zhou, K. Kanoda, and T.-K. Ng, Rev. Mod. Phys. **89**, 025003 (2017).

[2] L. Savary and L. Balents, Rep. Prog. Phys. **80**, 016502 (2017).

[3] C. Nayak, S. H. Simon, A. Stern, M. Freedman, and S. Das Sarma, Rev. Mod. Phys. **80**, 1083 (2008).

[4] V. Kalmeyer and R. B. Laughlin, Phys. Rev. Lett. **59**, 2095 (1987).

[5] D. F. Schroeter, E. Kapit, R. Thomale, and M. Greiter, Phys. Rev. Lett. **99**, 097202 (2007).

[6] R. Thomale, E. Kapit, D. F. Schroeter, and M. Greiter, Phys. Rev. B **80**, 104406 (2009).

[7] M. Greiter, D. F. Schroeter, and R. Thomale, Phys. Rev. B **89**, 165125 (2014).

[8] T. Meng, T. Neupert, M. Greiter, and R. Thomale, Phys. Rev. B **91**, 241106 (2015).

[9] Y.-C. He, D. N. Sheng, and Y. Chen, Phys. Rev. Lett. **112**, 137202 (2014).

[10] B. Bauer, L. Cincio, B. P. Keller, M. Dolfi, G. Vidal, S. Trebst, and A. W. W. Ludwig, Nat. Commun. **5**, 5137 (2014).

[11] S.-S. Gong, W. Zhu, and D. N. Sheng, Sci. Rep. **4**, 6317 (2014).

[12] K. Kumar, K. Sun, and E. Fradkin, Phys. Rev. B **90**, 174409 (2014).

[13] S.-S. Gong, W. Zhu, L. Balents, and D. N. Sheng, Phys. Rev. B **91**, 075112 (2015).

[14] A. Wietek, A. Sterdyniak, and A. M. Läuchli, Phys. Rev. B **92**, 125122 (2015).

[15] W. Zhu, S. S. Gong, and D. N. Sheng, Phys. Rev. B **94**, 035129 (2016).

[16] W.-J. Hu, W. Zhu, Y. Zhang, S. Gong, F. Becca, and D. N. Sheng, Phys. Rev. B **91**, 041124 (2015).

[17] S. Bieri, L. Messio, B. Bernu, and C. Lhuillier, Phys. Rev. B **92**, 060407 (2015).

[18] K. Kumar, K. Sun, and E. Fradkin, Phys. Rev. B **92**, 094433 (2015).

[19] A. E. B. Nielsen, G. Sierra, and J. I. Cirac, Nat. Commun. **4**, 2864 (2013).

[20] D. Poilblanc, J. I. Cirac, and N. Schuch, Phys. Rev. B **91**, 224431 (2015).

[21] X.-J. Liu, Z.-X. Liu, K. T. Law, W. V. Liu, and T. K. Ng, New J. Phys. **18**, 035004 (2016).

[22] C. Hickey, L. Cincio, Z. Papić, and A. Paramekanti, Phys. Rev. Lett. **116**, 137202 (2016).

[23] W.-J. Hu, S.-S. Gong, and D. N. Sheng, Phys. Rev. B **94**, 075131 (2016).

[24] A. Wietek and A. M. Läuchli, Phys. Rev. B **95**, 035141 (2017).

[25] X. G. Wen, F. Wilczek, and A. Zee, Phys. Rev. B **39**, 11413 (1989).

[26] X. G. Wen, Phys. Rev. B **44**, 2664 (1991).

[27] Y. Zhang, T. Grover, and A. Vishwanath, Phys. Rev. B **84**, 075128 (2011).

[28] Y. Zhang, T. Grover, A. Turner, M. Oshikawa, and A. Vishwanath, Phys. Rev. B **85**, 235151 (2012).

[29] X. Chen, Z.-C. Gu, Z.-X. Liu, and X.-G. Wen, Science **338**, 1604 (2012).

[30] Y.-M. Lu and A. Vishwanath, Phys. Rev. B **86**, 125119 (2012).

[31] T. Senthil and M. Levin, Phys. Rev. Lett. **110**, 046801 (2013).

[32] M. Barkeshli, arXiv:1307.8194.

[33] N. Regnault and T. Senthil, Phys. Rev. B **88**, 161106 (2013).

[34] A. Sterdyniak, N. R. Cooper, and N. Regnault, Phys. Rev. Lett. **115**, 116802 (2015).

[35] Y.-C. He, S. Bhattacharjee, F. Pollmann, and R. Moessner, Phys. Rev. Lett. **115**, 267209 (2015).

[36] R. Moessner and S. L. Sondhi, Phys. Rev. Lett. **86**, 1881 (2001).

[37] A. V. Chubukov, T. Senthil, and S. Sachdev, Phys. Rev. Lett. **72**, 2089 (1994).

[38] S. R. White, Phys. Rev. Lett. **69**, 2863 (1992).

[39] S. R. White, Phys. Rev. B **48**, 10345 (1993).

[40] L. Messio, C. Lhuillier, and G. Misguich, Phys. Rev. B **83**, 184401 (2011).

[41] I. Martin and C. D. Batista, Phys. Rev. Lett. **101**, 156402 (2008).

[42] Y. Kato, I. Martin, and C. D. Batista, Phys. Rev. Lett. **105**, 266405 (2010).

[43] A. Rahmani, R. A. Muniz, and I. Martin, Phys. Rev. X **3**, 031008 (2013).

[44] S. Jiang, A. Mesaros, and Y. Ran, Phys. Rev. X **4**, 031040 (2014).

[45] O. I. Motrunich, Phys. Rev. B **73**, 155115 (2006).

[46] F. D. M. Haldane, Phys. Rev. Lett. **61**, 2015 (1988).

[47] G. Jotzu, M. Messer, R. Desbuquois, M. Lebrat, T. Uehlinger, D. Greif, and T. Esslinger, Nature (London) **515**, 237 (2014).

[48] M. Claassen, H.-C. Jiang, B. Moritz, and T. P. Devereaux, arXiv:1611.07964.

[49] S. Kitamura, T. Oka, and H. Aoki, Phys. Rev. B **96**, 014406 (2017).

[50] B. Bernu, C. Lhuillier, and L. Pierre, Phys. Rev. Lett. **69**, 2590 (1992).

[51] B. Bernu, P. Lecheminant, C. Lhuillier, and L. Pierre, Phys. Rev. B **50**, 10048 (1994).

[52] G. M. Crosswhite, A. C. Doherty, and G. Vidal, Phys. Rev. B **78**, 035116 (2008).

[53] I. P. McCulloch, arXiv:0804.2509.

[54] L. Cincio and G. Vidal, Phys. Rev. Lett. **110**, 067208 (2013).

[55] P. Zanardi and N. Paunković, Phys. Rev. E **74**, 031123 (2006).

[56] S.-J. Gu, Int. J. Mod. Phys. B **24**, 4371 (2010).

[57] R. Orús, Ann. Phys. **349**, 117 (2014).

[58] A. Thomson and S. Sachdev, Phys. Rev. B **95**, 205128 (2017).

[59] Y. Machida, S. Nakatsuji, S. Onoda, T. Tayama, and T. Sakakibara, Nature (London) **463**, 210 (2010).

[60] Y. Iqbal, T. Müller, K. Riedl, J. Reuther, S. Rachel, M. Valentí, M. J. P. Gingras, R. Thomale, and H. O. Jeschke, arXiv:1705.05291.

[61] M. Greiter and R. Thomale, Phys. Rev. Lett. **102**, 207203 (2009).

[62] B. Scharfenberger, R. Thomale, and M. Greiter, Phys. Rev. B **84**, 140404 (2011).

[63] Z.-X. Liu, H.-H. Tu, Y.-H. Wu, R.-Q. He, X.-J. Liu, Y. Zhou, and T.-K. Ng, arXiv:1509.00391.

[64] P. Lecheminant and A. M. Tsvelik, Phys. Rev. B **95**, 140406 (2017).

[65] S. N. Saadatmand and I. P. McCulloch, Phys. Rev. B **96**, 075117 (2017).

[66] S.-S. Gong, W. Zhu, J.-X. Zhu, D. N. Sheng, and K. Yang, Phys. Rev. B **96**, 075116 (2017).